Channel Model of Line-of-Sight Radio Propagation by Reflection over Lossy Ground for Cellular Networks

Zoran Blažević, Maja Škiljo, and Dragan Poljak

***Abstract*—In this paper, we propose the radio channel model for propagation by reflection over realistic ground. The formulas for electromagnetic field strength, power density, received power, and path-gain are derived for arbitrary oriented antennas. The results obtained by the proposed model in an example of a vertical half-wave dipole above real ground transmitting at a 5G frequency are first validated by full-wave model results and discussed upon. Also, the dosimetry parameters for human exposure at a 5G frequency are inspected for radiated power of 100 W and different transmitter heights. Finally, the power received by a half-wave dipole is calculated.**

***Index Terms*—radio-propagation over ground, incident field strength, incident power density, path-gain.**

I. Introduction

The contemporary development of cellular networks, aimed at satisfying an increasing number of services and users [1], places new demands on network planning opening new issues in electromagnetic compatibility (EMC) and exposure dosimetry [2], [3]. In order to build a radio network that ensures good Quality-of-Service (QoS) and that, at the same time, obeys EMC and exposure limits, proper estimation and characterization of the received field strength and power are of the outermost importance. For that purpose, extensive radio measurements and complex simulation tools are commonly used.

As in classic cellular networks the mobile receiver is usually in the radio shadow (of buildings, etc.), their physical layer is characterized statistically, as in [4], with the possibility to estimate the mean power and path-loss law analytically as in [5]. Examples of the radio-channel characterization in new generations of the networks can be found in, e.g., [6], [1].

However, new generations of mobile networks (5G/6G) will also result in a larger number of base station antennas erected at lower or moderate heights serving nearby users with a clear Line-of-Sight (LOS) path to their devices [3]. In such scenarios, the received field pattern is shaped mostly by the energy arriving via a direct path and a ground-reflected path, whereas the diffuse multipath component can be expected to be rather small. Then, a quite accurate prediction of the received signal strengths is possible to obtain analytically.

However, the often used classic far-field model for radio-propagation by reflection over ground from [7] (Eq. (3.37)) or [8] may not be fully adequate for the purpose when dealing with cellular networks. On the other hand, the influence of the ground should not be neglected (as often done, e.g., in [9] for near field) by relying solely on the Fris formula for the free-space propagation [10]. Furthermore, although it accounts for the impact of the antenna radiation pattern on the direct and ground-reflected field, the enhanced model of [11], [12] does not fully take into account their different angles of arrival to the receiving point.

Therefore, in this paper, we propose an analytical approach to the analysis of the LOS radio propagation over ground based on ray-tracing method, including the scenarios where the antennas' heights are comparable to their mutual separation. This analytical model can provide a quick assessment of the radio channel and dosimetry parameters, for various situations using different frequencies, polarizations, radiated powers, antennas' heights and radiation patterns. Besides antenna characteristics and propagation geometry, the proposed two-path model takes into account the properties of soil through Fresnel's reflection coefficients, resulting in an excellent agreement with the numerical results calculated by 4nec2 software.

The two-path model approach adopted herein showed to be rather effective prediction tool in practical radio measurements, e.g. for WiFi-based Long Distance (WiLD) networks [13]. It is also used as a channel model for Vehicular Ad-Hoc Networks in [14]. However, the applied approximation of parallel propagation paths applied there does not hold when the antenna separations are comparable to the antenna heights. Such scenarios occur frequently in cellular networks, and the model extensions that provide a remedy taking into account the accurate field vector sum are worked out in this paper. It is an extension of our conference paper [15] with further development of the model. Herein, we derive the relations for the power received by a directional antenna and upgrade the proposed path-loss model accordingly. Also, a more detailed discussion is provided along with some additional results.

The paper is organized as follows. In Sec. II, based on

Manuscript received October 31, 2025; revised December 17, 2025. Date of publication January 12, 2026. Date of current version January 12, 2026. The associate editor prof. Giovanna Calò has been coordinating the review of this manuscript and approved it for publication.

Authors are with the University of Split, Faculty of Electrical Engineering, Mechanical Engineering and Naval Architecture, Split, Croatia (e-mails: zblaz@fesb.hr, msekelja@fesb.hr, dpoljak@fesb.hr).

The paper was presented in part at the International Conference on Smart and Sustainable Technologies (SpliTech) 2025.

This work was supported by the Croatian Science Foundation under the project number HRZZ-IPS-2024-02-7779.

Digital Object Identifier (DOI): 10.24138/jcomss-2025-0232

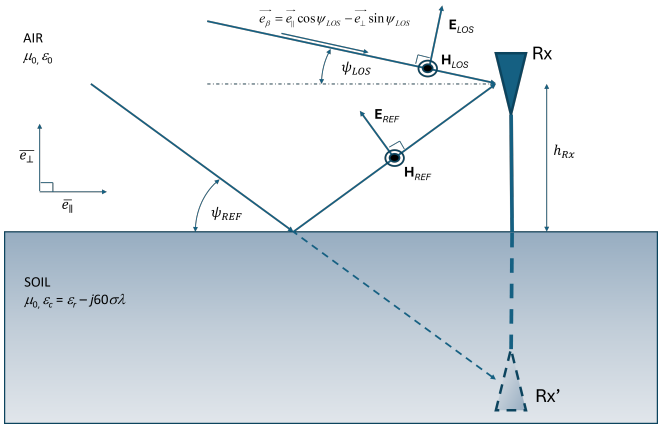

Fig. 1. Vertically (TM) polarized EM field incidence above lossy ground.

the ray-tracing method and modified image theory, the full two-path channel model for the wave propagation over arbitrary soil is derived for vertically and horizontally polarized electromagnetic (EM) fields. The proposed model is verified by a detailed analysis of an example of a vertical half-wave (electric and magnetic) straight dipole transmitter radiating at a 5G frequency above ground in Sec. III, whereas Sec. IV concludes the paper.

II. Electromagnetic Field of Dipole Above Ground

The strength of the electric field (in volts per meter) in free space at a distance r far from the transmitter with the gain pattern $G_{Tx} = G_{Tx}(\psi)$ that radiates the power P_{Tx} (in watts) is given by [7]:

$$E = \sqrt{\frac{Z_0 P_{Tx} G_{Tx}}{4\pi}} \frac{1}{r} \tag{1}$$

where $Z_0 = 120\pi\ \Omega$ is the free-space impedance. The magnetic field strength in the far zone of the transmitter is simply $H = \frac{E}{Z_0}$. The fields propagate through space as $\boldsymbol{E}, \boldsymbol{H} \propto e^{-j\beta r}$, $\beta = \frac{2\pi}{\lambda} = \frac{2\pi f}{c}$, c being the velocity of light and λ is the wavelength.

Let us now consider the radiation in far-field at a frequency f of a matched dipole settled at a height $h_{Tx} >> \lambda$ above infinite real soil of permittivity ϵ_r and conductivity σ. Following Fig. 1, the incident field at the observed point T in the upper space is the sum of two components:

$$\vec{\boldsymbol{E}}(T) = \vec{\boldsymbol{E}}_{LOS}(T) + \vec{\boldsymbol{E}}_{REF}(T) \tag{2}$$

where, applying (1), $\vec{\boldsymbol{E}}_{LOS}(T) = \vec{\boldsymbol{E}}(\vec{r_0})$ is the direct wave component and $\vec{\boldsymbol{E}}_{REF}(T) = \vec{\boldsymbol{E}}(\vec{r_i})$ is the reflected wave component. Here, r_0 and r_i are the radio path lengths of the direct and the reflected wave, respectively, $r_{0,i} = \sqrt{d^2 + (h_{Tx} \mp h_{Rx})^2}$, d being the lateral distance from the transmitter. The angles of arrival of the incoming rays $\psi = \psi_{LOS,REF}$ are measured as $\sin\psi_{LOS,REF} = \frac{h_{Tx} \mp h_{Rx}}{r_{0,i}}$.

The reflected field can be calculated applying modified image theory and Fresnel reflection coefficients R_H and R_V for perpendicular (horizontal or transversally electric (TE)) polarization and for parallel (vertical or transversally magnetic (TM)) polarization, respectively. In the case of flat smooth ground in Fig. 1, they can be expressed as [7]:

$$R_H = \frac{\sin\psi_{REF} - \sqrt{\epsilon_c - \cos^2\psi_{REF}}}{\sin\psi_{REF} + \sqrt{\epsilon_c - \cos^2\psi_{REF}}} \tag{3}$$

$$R_V = \frac{\epsilon_c \sin\psi_{REF} - \sqrt{\epsilon_c - \cos^2\psi_{REF}}}{\epsilon_c \sin\psi_{REF} + \sqrt{\epsilon_c - \cos^2\psi_{REF}}} \tag{4}$$

where $\epsilon_c = \epsilon_r - j60\sigma\lambda$ is the complex permittivity of soil. The roughness and curvature of the ground surface can also be included in the calculation, according to the Rayleigh criterion and applying the divergence factor, respectively [7] .

A. Vertically polarized wave

Accounting for the field components parallel to the ground and the perpendicular ones while applying (2) and the modified image theory, the strength of the vertically polarized total electric field above ground can be expressed as:

$$E^V_{Rx} = g^V_\parallel \sqrt{\frac{Z_0 P_{Tx} G^V_{Tx}(\psi_{LOS})}{4\pi}} \frac{1}{r_0} \tag{5}$$

where, in the case of parallel polarization, the influence of the ground on the total electric field is expressed by the parameter:

$$g^V_\parallel = \sqrt{1 + 2\kappa_V Re\left(R_V e^{-j\beta\Delta}\right)\cos\left(\psi_{LOS} + \psi_{REF}\right) + \kappa_V^2 |R_V|^2} \tag{6}$$

in which $\Delta = r_i - r_0$, and:

$$\kappa_V = \frac{r_0 G^V_{Tx}(\psi_{REF})}{r_i G^V_{Tx}(\psi_{LOS})} \tag{7}$$

where G^V_{Tx} refers to the vertically polarized antenna radiation pattern. In a sense, the parameter κ_V weights the contribution of the field component reflected from the soil to the total field relative to the antenna radiation pattern and the receiver height.

Applying (2), the total electric field at the observed point above ground is found to be oriented in the direction of the complex unit vector:

$$\begin{aligned}\vec{e}_V = \frac{1}{g^V_\parallel}\{&\left[\sin\psi_{LOS} - \kappa_V R_V \sin\psi_{REF} e^{-j\beta\Delta}\right]\vec{e}_\parallel \\ &+ \left[\cos\psi_{LOS} + \kappa_V R_V \cos\psi_{REF} e^{-j\beta\Delta}\right]\vec{e}_\perp\}\end{aligned} \tag{8}$$

At the same time, the total magnetic field at the observation point is perpendicular to the incident plane (in direction of ort vector $\vec{n} = \vec{e}_\parallel \times \vec{e}_\perp$) and its strength can be expressed as:

$$H^V_{Rx} = g^V_\perp \sqrt{\frac{P_{Tx} G^V_{Tx}(\psi_{LOS})}{4\pi Z_0}} \frac{1}{r_0} \tag{9}$$

where, in the case of parallel polarization, the influence of the ground on the total magnetic field is expressed by the parameter:

$$g^V_\perp = \sqrt{1 + 2\kappa_V Re\left(R_V e^{-j\beta\Delta}\right) + \kappa_V^2 |R_V|^2} \tag{10}$$

The intrinsic impedance of the upper half-space in the case of vertically polarized incident field is $Z_i^V = \frac{E_{Rx}^V}{H_{Rx}^V} = \frac{g_\parallel^V}{g_\perp^V} Z_0$.

Considering that the electric and magnetic fields are mutually perpendicular, the power density at the observed point can be expressed as:

$$S^V = E_{Rx}^V H_{Rx}^V = G_G^V \frac{P_{Tx} G_{Tx}^V(\psi_{LOS})}{4\pi r_0^2} \tag{11}$$

where $G_G^V = g_\parallel^V g_\perp^V$.

B. Horizontally polarized wave

The analysis for the case of horizontal polarization follows the same procedure as for the vertical one. The horizontally polarized electric field is in the direction of the ort vector $-\vec{n}$, and its strength is:

$$E_{Rx}^H = g_\perp^H \sqrt{\frac{Z_0 P_{Tx} G_{Tx}^H(\psi_{LOS})}{4\pi}} \frac{1}{r_0} \tag{12}$$

where:

$$g_\perp^H = \sqrt{1 + 2\kappa_H Re\left(R_H e^{-j\beta\Delta}\right) + \kappa_H^2 |R_H|^2} \tag{13}$$

Here, G_{Tx}^H refers to the horizontally polarized antenna radiation pattern and:

$$\kappa_H = \frac{r_0 G_{Tx}^H(\psi_{REF})}{r_i G_{Tx}^H(\psi_{LOS})} \tag{14}$$

The total magnetic field is in the direction of the unit vector:

$$\begin{aligned}\vec{e}_H = \frac{1}{g_\parallel^H} \{ &\left[\sin\psi_{LOS} - \kappa_H R_H \sin\psi_{REF} e^{-j\beta\Delta}\right] \vec{e}_\parallel \\ &+ \left[\cos\psi_{LOS} + \kappa_H R_H \cos\psi_{REF} e^{-j\beta\Delta}\right] \vec{e}_\perp \}\end{aligned} \tag{15}$$

where:

$$g_\parallel^H = \sqrt{1 + 2\kappa_H Re\left(R_H e^{-j\beta\Delta}\right)\cos\left(\psi_{LOS} + \psi_{REF}\right) + \kappa_H^2 |R_H|^2} \tag{16}$$

The horizontally polarized total magnetic field strength can be expressed as:

$$H_{Rx}^H = g_\parallel^H \sqrt{\frac{P_{Tx} G_{Tx}^H(\psi_{LOS})}{4\pi Z_0}} \frac{1}{r_0} \tag{17}$$

The intrinsic impedance of the upper half-space in the case of horizontally polarized incident field is $Z_i^H = \frac{E_{Rx}^H}{H_{Rx}^H} = \frac{g_\perp^H}{g_\parallel^H} Z_0$.

The power density of the horizontally polarized wave is given by:

$$S^H = E_{Rx}^H H_{Rx}^H = G_G^H \frac{P_{Tx} G_{Tx}^H(\psi_{LOS})}{4\pi r_0^2} \tag{18}$$

where $G_G^H = g_\perp^H g_\parallel^H$.

C. Received power

With knowledge of the incident power density via (11), (18), the power absorbed by an omnidirectional antenna with directivity gain $G_{Rx}^{V,H} = const.$ in the incident plane can be represented as:

$$\begin{aligned}P_{Rx,omni}^{V,H} &= \frac{\lambda^2}{4\pi} G_{Rx}^{V,H} S^{V,H} \\ &= P_{Tx} G_{Tx}^{V,H}(\psi_{LOS}) G_{Rx}^{V,H} G_G^{V,H} \left(\frac{\lambda}{4\pi r_0}\right)^2\end{aligned} \tag{19}$$

where the indices V and H refer to vertical (parallel) and horizontal (perpendicular) polarization, respectively.

Depending on polarization, the direction of arrival of the power at the receiving antenna is determined (using (8), (15) and Fig. 1) by the unit vector:

$$\begin{aligned}\vec{e}_S^{V,H} &= \vec{e}_{V,H} \times \vec{n} \\ &= \frac{1}{g_\parallel^{V,H}} \left(\vec{e}_\beta + \kappa_{V,H} R_{V,H} e^{-j\beta\Delta} \vec{e}_g\right)\end{aligned} \tag{20}$$

where: $\vec{e}_\beta = \cos\psi_{LOS}\vec{e}_\parallel - \sin\psi_{LOS}\vec{e}_\perp$ and $\vec{e}_g = \cos\psi_{REF}\vec{e}_\parallel + \sin\psi_{REF}\vec{e}_\perp$ are the unit vectors in the direction of the direct wave and the wave reflected from the ground, respectively (see Fig. 1) .

However, as the EM energy arrives at the receiving antenna from the two different directions, the total power absorbed by the conjugate matched antenna with arbitrary gain pattern $G_{Rx}^{V,H} = G_{Rx}^{V,H}(\psi)$ can be calculated allowing for both transmitter and receiver gain patterns to equally shape the contribution of different radio-paths as:

$$P_{Rx}^{V,H} = P_{Tx} G_{Tx}^{V,H}(\psi_{LOS}) G_{Rx}^{V,H}(\psi_{LOS}) \Gamma_G^{V,H} \left(\frac{\lambda}{4\pi r_0}\right)^2 \tag{21}$$

where:

$$\Gamma_G^{V,H} = \gamma_\perp^{V,H} \gamma_\parallel^{V,H} \tag{22}$$

in which:

$$\gamma_\perp^{V,H} = \sqrt{1 + 2K_{V,H} Re\left(R_{V,H} e^{-j\beta\Delta}\right) + K_{V,H}^2 |R_{V,H}|^2} \tag{23}$$

$$\gamma_\parallel^{V,H} = \sqrt{\begin{aligned}&1 + K_{V,H}^2 |R_{V,H}|^2 \\ &+2K_{V,H} Re\left(R_{V,H} e^{-j\beta\Delta}\right)\cos\left(\psi_{LOS} + \psi_{REF}\right)\end{aligned}} \tag{24}$$

In (21)-(24) the influence of the ground is reshaped relative to (19) by the factor $K_{V,H}$ that, respecting (7), (14), can be written as:

$$\begin{aligned}K_{V,H} &= \kappa_{V,H} \frac{G_{Rx}^{V,H}(\psi_{REF})}{G_{Rx}^{V,H}(\psi_{LOS})} \\ &= \frac{r_0 G_{Tx}^{V,H}(\psi_{REF}) G_{Rx}^{V,H}(\psi_{REF})}{r_i G_{Tx}^{V,H}(\psi_{LOS}) G_{Rx}^{V,H}(\psi_{LOS})}\end{aligned} \tag{25}$$

Note that, when the receiver is an omnidirectional antenna in the incident plane, $\gamma_{\parallel,\perp}^{V,H} = g_{\parallel,\perp}^{V,H}$, i.e., $\Gamma_G^{V,H} = G_G^{V,H}$.

D. Path gain

Respecting the previous considerations while using (21), the total path gain for radio channels over ground can be expressed as:

$$\begin{aligned} G^{V,H} &= \frac{P_{Rx}^{V,H}}{P_{Tx}^{V,H}} \\ &= G_{FS}\Gamma_G^{V,H} G_{Tx}^{V,H}\left(\psi_{LOS}\right) G_{Rx}^{V,H}\left(\psi_{LOS}\right) \end{aligned} \tag{26}$$

where G_{FS} is the free-space path gain when both antennas have the directivity gain pattern equal to that of the isotropic radiator.

In decibels, expressing $\Gamma_G^{V,H} = G_{FF}^{V;H} G_{NF}^{V;H}$, it is given by:

$$\begin{aligned} G^{V,H}(dB) = G_{FS}(dB) + G_{FF}^{V,H}(dB) + G_{NF}^{V,H}(dB) \\ + G_{Tx}^{V,H}(dB) + G_{Rx}^{V,H}(dB) \end{aligned} \tag{27}$$

where $G_{Tx}^{V,H}(dB) = 10\log G_{Tx}^{V,H}\left(\psi_{LOS}\right)$, $G_{Rx}^{V,H}(dB) = 10\log G_{Rx}^{V,H}\left(\psi_{LOS}\right)$, and:

$$\begin{aligned} G_{FS}(dB) &= 20\log\frac{\lambda}{4\pi r_0} \\ &= -32.45 - 20\log f_{GHz} - 20\log r_0 \end{aligned} \tag{28}$$

is the Fris equation for the isotropic antennas where f_{GHz} is the frequency in gigahertz,

$$G_{FF}^{V,H}(dB) = 10\log\left[1 + 2K_{V,H}Re\left(R_{V,H}e^{-j\beta\Delta}\right) + K_{V,H}^2|R_{V,H}|^2\right] \tag{29}$$

$$G_{NF}^{V,H}(dB) = 5\log\left[1 - \frac{2K_{V,H}Re\left(R_{V,H}e^{-j\beta\Delta}\right)\left[1-\cos\left(\psi_{LOS}+\psi_{REF}\right)\right]}{1 + 2K_{V,H}Re\left(R_{V,H}e^{-j\beta\Delta}\right) + K_{V,H}^2|R_{V,H}|^2}\right] \tag{30}$$

The factor $G_{FF}^{V,H}$ dominates at long distances and depicts the radio propagation of the far field. On the other hand, $G_{NF}^{V,H}$ has an impact on the radiation near-field of the antenna above ground where the antenna separations d are comparable to their heights, and it vanishes at very large distances from the transmitter where $d >> h_{Tx}, h_{Rx}$. Then, the incident angle ψ_{REF} is small, therefore in the case of real ground: $R_{V,H} \approx -1$, $K_{V,H} \approx 1$ and (30) reduces to $G_{FF}^{V,H} \approx 4\sin^2\frac{\beta\Delta}{2}$.

Furthermore, in that case, after considering the Taylor series expansion of the path difference it is found that $\Delta \approx \frac{2h_{Tx}h_{hx}}{d}$, and the last local maximum of $G_{FF}^{V,H}$ is found to be at the distance $d_{max} = \frac{4h_{Tx}h_{hx}}{\lambda}$. Beyond this point, it decreases as $G_{FF}^{V,H} \approx \left(\frac{4\pi h_{Tx}h_{hx}}{d\lambda}\right)^2$, which is essentially the result already given in [7]. Given that it is multiplied in (26) by G_{FS} which decreases with the square of distance (see (28)), the total radio gain $G^{V,H}$ drops with the fourth power of distance in the far zone. For the same reason, unless the antenna gain patterns vary in frequency, it is also independent on frequency there.

It should be noted that the factor $\Gamma_G^{V,H}$ in (26), (27) shows a dependence on the antennas' radiation patterns (through the factor $K_{V,H}$). Thus, in the sense of the classic digital radio channel block scheme given in [16], there is not always a clear distinction between the propagation channel and the antennas in the radio channel in this case. According to (23), (24), and (25), unless the antennas are omnidirectional in the incident plane, they can be distinguished only in the far zone of the transmitter when $K_{V,H} \approx \kappa_{V,H} \approx \frac{r_0}{r_i}$. This condition is not always fulfilled in cellular networks. Therefore, the proposed model offers a straightforward approach to address some of the network design issues raised in [10].

If necessary, besides the introduction of ground roughness in (3), (4), the proposed model can be easily upgraded by additional gain factors in (26), i.e. in (27), such as rain attenuation or attenuation caused by water vapor and oxygen in the atmosphere. In addition, the radiopath lengths r_0 and r_i can be estimated allowing for tropospheric refraction [7]. Note that existing path-loss models depicting more complex propagation scenarios, such as in [17], can be easily upgraded by this model.

Of course, the main limitation of the proposed model stems from the Fresnel reflection coefficient approximation to the Sommerfeld solution, i.e. it is tied to the antenna height relative to the signal wavelength. More about that can be found in [18]. However, it is safe to say that whenever the antenna heights above ground are greater than a wavelength, the error will be negligible. This is confirmed in Figs. 2, 3. given in the section that follows.

III. Vertical dipole above ground

Let us now take a typical example of a vertical half-wave (electric or magnetic) dipole radiating the power $P_{Tx} = 100$ W at a 5G frequency of $f = 3.6$ GHz. It is erected at a height $h_{Tx} = 8$ m above flat lossy ground. Following [19], its directive gain pattern can be expressed as:

$$G_{Tx}^{V,H} = 1.64\frac{\cos^2\left(\frac{\pi}{2}\sin\psi\right)}{\cos^2\psi} \tag{31}$$

where the launch angle ψ is measured relative to the line perpendicular to the antenna axis, which is parallel to the ground and in the direction of maximum radiation.

The soil permittivity at the selected frequency is taken to be $\varepsilon_r = 4$, and the conductivity $\sigma = 3\cdot 10^{-3}$ S/m. As $\varepsilon_r >> 60\sigma\lambda$, the soil behaves as a low-loss dielectric.

First, in order to validate the proposed analytical model for radio-propagation over ground, we verify the results of the received electric field strength at a distance d of 10 m from the half-wave electric dipole calculated by (5) with the results of the full-wave model obtained by 4nec2 using the Method of Moments and Sommerfeld solution in Fig. 2. In 4nec2, a 4.15 cm long straight wire with a radius of 0.1 mm fed at the center is used to simulate the transmitter. There is excellent agreement between the analytical and numerical results. The field strength varies in an oscillatory manner with the height showing a quasi-linear trend of increasing as the distance from the antenna becomes less.

Next, the model is tested for the results of the vertically polarized electric field strength versus the distance from the transmitter. The results are depicted in Fig. 3. Again, there is excellent agreement between the results. As expected, the field varies in an oscillatory manner with the distance from the transmitter. First, it shows a trend of increasing as the receiving

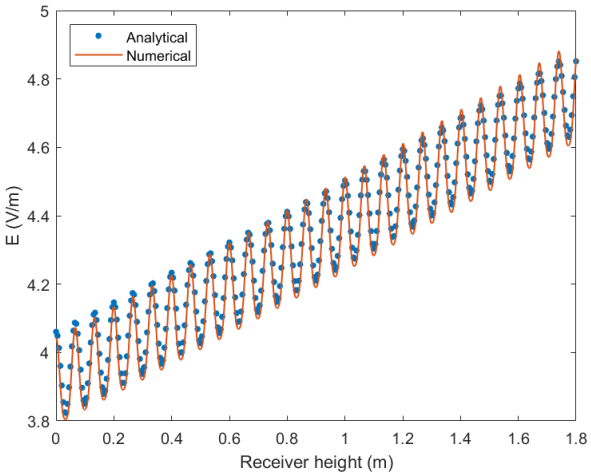

Fig. 2. Comparison between analytical and numerical results for the received electric field above ground 10 meters from the dipole (vertical polarization)

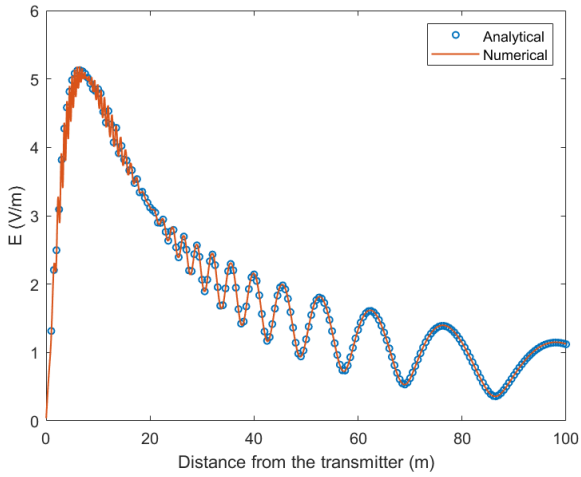

Fig. 3. Comparison between analytical and numerical results for the received electric field 1.8 m above ground versus distance from the dipole erected at 8-m height (vertical polarization)

point enters the antenna beam and then, after approximately eight meters, it starts to decrease oscillatory.

The received electric field normalized to the strength of the electric field in free space versus the distance from the transmitter is given in Fig. 4 in the cases of the half-wave electric dipole transmitter (vertical polarization) and of the half-wave magnetic dipole transmitter (horizontal polarization). The oscillations of the field strength are more emphasized for horizontal polarization, which is caused by the difference between the reflection coefficients.

By distance of somewhwere about $d = h_{Tx} + h_{Rx} = 9.8$ m, the horizontally polarized and vertically polarized fields vary in phase with the distance. Inside that area, the component parallel to the ground of the vertically polarized electric field incident to the ground prevails over the perpendicular one. According to the image theory, it reflects in counter-phase with the incident wave component parallel to the ground, similarly as the ground-reflected component of the horizontally

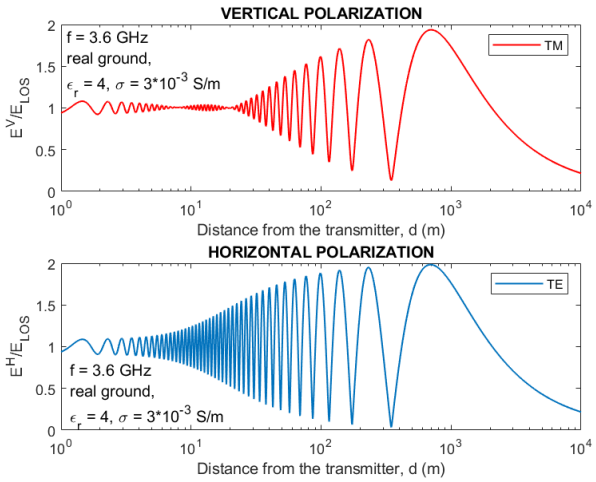

Fig. 4. Normalized electric field over ground vs. distance from the transmitter

polarized electric field does.

As the receiving point departs further from that distance, the incident field component perpendicular to the ground that is in phase with the direct wave prevails. The horizontally polarized and vertically polarized fields then start to vary in counter-phase until the point of the pseudo-Brewster angle $\psi_B = \arcsin \frac{1}{\sqrt{1+\varepsilon_c}}$ is reached at approximately 20 m from the transmitter, where the reflected field is minimum (see (4)). Beyond that distance, because of the change in phase of the reflected field when the incident angle becomes less than the pseudo-Brewster one, they commence to vary in phase again.

By approaching the position of the last maximum, the oscillations of the field become maximal (between zero and twice the free-space field strength). This position is equal in both cases (as expected) showing that, for the receiver at a height of 1.8 m, the 3.6-GHz far-field of the dipole erected eight meters over ground begins at $d = d_{max} = \frac{4h_{Tx}h_{hx}}{\lambda} = 692$ m. At larger distances, $d > d_{max}$, the field strength decays as $E_{Rx} \propto d^{-2}$, and the received power as $P_{Rx} \propto E_{Rx}^2 \propto d^{-4}$ [7]. This is in accordance with the discussion on the far-field radio gain from Sec. II.D.

In addition to network optimization, accurate predictions of the incident field strength are also very important for reliable EM dosimetry. Besides the incident field being one of the dosimetry parameters itself [20], it is an input parameter for the calculation of other exposure parameters such as the incident power density (see (11), (18)), the in-body induced electric field, etc. [2]. However, following ICNIRP [20], it is not applicable to the selected 5G frequency. An applicable one is the incident power density, for which the reference level for exposure to electromagnetic fields at $f > 2$ GHz averaged over 30 min and over the whole body is 10 W/m^2 for general population and 50 W/m^2 for occupational.

The incident power density against the distance from the transmitter calculated by (11) for the selected scenario is given in Fig. 5 for both polarizations. In addition to distance, it is vividly governed by the properties of the ground and antenna radiation pattern. The maximum power density is at

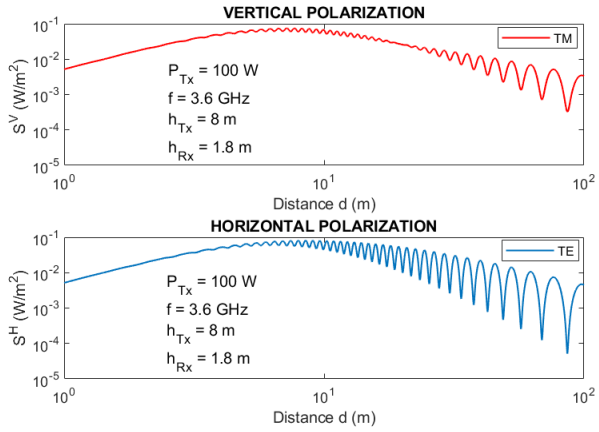

Fig. 5. Incident power density vs. distance from the transmitter erected at height of 8 m

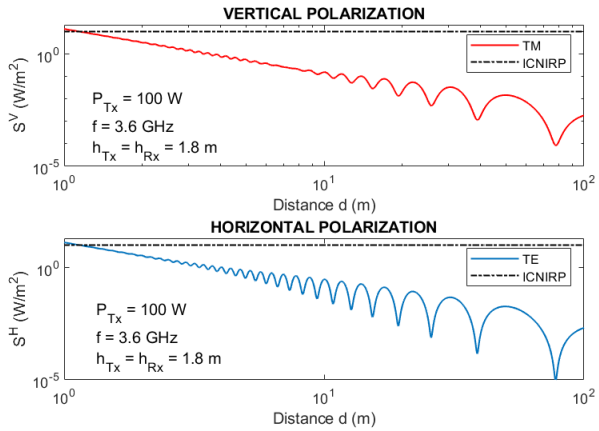

Fig. 6. Incident power density vs. distance from the transmitter erected at height of 1.8 m

the distance of approximately eight meters from the transmitter, exhibiting more oscillatory behavior as the distance increases. The values obtained are found to be well below the exposure limits. However, the power density oscillations should be considered when measuring the total exposure in real environments.

To assess the impact of the antenna radiation pattern in combination with the transmitter height, we checked the same scenario, but of the dipole at height $h_{Tx} = h_{Rx} = 1.8$ m where $G_{Tx}^{V,H}(\psi_{LOS} = 0) = 1.64 = 2.15$ dBi. The results are shown in Fig. 6. In this case, however, the power density has a continuous trend of decreasing with distance. For the radiated power of $P_{Tx} = 100$ W, regardless of the polarization, the exposure limit for general public is exceeded in the antenna vicinity up to more than a meter from.

Finally, the power received by a conjugate matched vertical half-wave dipole 1.8 m above real ground versus antenna separation is calculated by (21) and given in Fig. 7. Because of the shape of the dipole radiation pattern, the power received immediately below the transmitter antenna is zero and increases as the receiver departs from the transmitter by a distance of approximately 10 m. Beyond this distance,

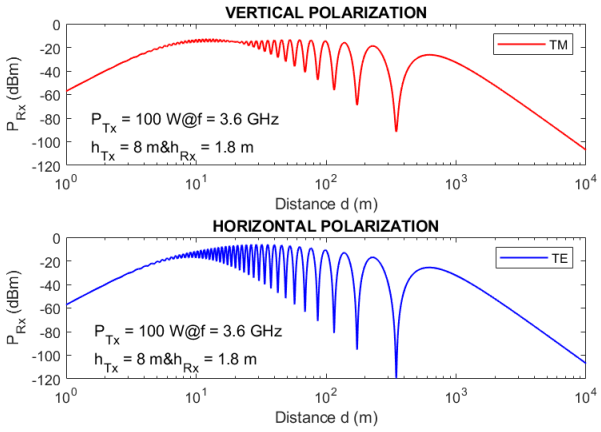

Fig. 7. Power received by matched half-wave receiver above real soil

the received power decreases, increasing the intensity of the oscillations until the last local maximum at $d = d_{max}$ is reached, after which it continuously drops with the fourth power of the distance.

IV. Conclusion

The proposed channel model for radio-propagation over realistic ground ensures reliable predictions of the channel parameters and dosimetry in all cases where the soil is out of the near-field region of the antennas, and it can be easily upgraded by additional gain factors if needed. As such, it can be well applied to the characterization of LOS radio channels in cellular and radio networks of other types in similar scenarios. With some caution necessary due to the Fresnel approximation for the Sommerfeld reflection coefficients, it could also be tested for the transmitter in greater proximity to the ground. However, we are leaving this matter for future considerations.

Acknowledgment

This work was supported by the Croatian Science Foundation under the project number HRZZ-IPS-2024-02-7779.

References

[1] T. S. Rappaport, S. Sun, R. Mayzus, H. Zhao, Y. Azar, K. Wang, G. N. Wong, J. K. Schulz, M. Samimi, and F. Gutierrez, "Millimeter wave mobile communications for 5g cellular: It will work!" *IEEE Access*, vol. 1, pp. 335–349, 2013.

[2] L. Chiaraviglio, A. Elzanaty, and M.-S. Alouini, "Health risks associated with 5g exposure: A view from the communications engineering perspective," *IEEE Open Journal of the Communications Society*, vol. 2, pp. 2131–2179, 2021.

[3] W. H. Bailey, B. R. T. Cotts, and P. J. Dopart, "Wireless 5g radiofrequency technology — an overview of small cell exposures, standards and science," *IEEE Access*, vol. 8, pp. 140 792–140 797, 2020.

[4] H. Suzuki, "A statistical model for urban radio propogation," *IEEE Transactions on Communications*, vol. 25, no. 7, pp. 673–680, 1977.

[5] D. Chizhik and J. Ling, "Propagation over clutter: Physical stochastic model," *IEEE Transactions on Antennas and Propagation*, vol. 56, no. 4, pp. 1071–1077, 2008.

[6] V. R. F. Guijarro, J. D. Vega Sánchez, M. C. P. Paredes, F. G. Arévalo, and D. P. M. Osorio, "Comparative evaluation of radio network planning for different 5g-nr channel models on urban macro environments in quito city," *IEEE Access*, vol. 12, pp. 5708–5730, 2024.

[7] L. Boithias, *Radio Wave Propagation*. North Oxford Academic, 1987. [Online]. Available: https://books.google.hr/books?id=H62lQAAACAAJ
[8] T. S. Rappaport, *Wireless Communications: Principles and Practice*, 2nd ed. Cambridge University Press, 2024.
[9] M. S. Elbasheir, R. A. Saeed, and S. Edam, "Electromagnetic field exposure boundary analysis at the near field for multi-technology cellular base station site," *IET Communications*, vol. 18, no. 1, pp. 11–27, 2024. [Online]. Available: https://ietresearch.onlinelibrary.wiley.com/doi/abs/10.1049/cmu2.12711
[10] T. K. Sarkar, S. Burintramart, N. Yilmazer, S. Hwang, Y. Zhang, A. De, and M. Salazar-Palma, "A discussion about some of the principles/practices of wireless communication under a maxwellian framework," *IEEE Transactions on Antennas and Propagation*, vol. 54, no. 12, pp. 3727–3745, 2006.
[11] S. Loyka and A. Kouki, "Using two ray multipath model for microwave link budget analysis," *IEEE Antennas and Propagation Magazine*, vol. 43, no. 5, pp. 31–36, 2001.
[12] S. Loyka, A. Kouki, and F. Gagnon, "Fading prediction on microwave links for airborne communications," in *IEEE 54th Vehicular Technology Conference. VTC Fall 2001. Proceedings (Cat. No.01CH37211)*, vol. 4, 2001, pp. 1960–1964 vol.4.
[13] M. Rademacher, M. Kessel, and K. Jonas, "Experimental results for the propagation of outdoor ieee802.11 links," in *Mobilkommunikation - Technologien und Anwendungen. Vorträge der 21. ITG-Fachtagung, 11.-12. Mai 2016 in Osnabrück. ITG-Fachbericht, Bd. 263*, 2016, pp. 32 – 36. [Online]. Available: https://www.vde-verlag.de/proceedings-en/454220005.html
[14] A. Jaiswal, S. K. Singh, S. Kumar, B. B. Gupta, and K. T. Chui, "Advanced evaluation of propagation models and routing protocols in vehicular ad-hoc networks," in *2024 IEEE Cyber Science and Technology Congress (CyberSciTech)*, 2024, pp. 406–411.
[15] Z. Blažević, M. Škiljo, and D. Poljak, "Channel model of line-of-sight radio propagation by reflection over lossy ground for cellular networks," in *2025 10th International Conference on Smart and Sustainable Technologies (SpliTech)*, 2025, pp. 1–5.
[16] R. Steele, *Mobile Radio Communications*. Pentech Press, IEEE Press, 1992.
[17] J. Zang and S. Wang, "Path loss modeling and analysis for low antenna height over grass environment," in *2021 IEEE 4th International Conference on Electronic Information and Communication Technology (ICEICT)*, 2021, pp. 183–185.
[18] M. G. Cotton, E. F. Kuester, and C. L. Holloway, "An investigation into the geometric optics approximation for indoor scenarios with a discussion on pseudolateral waves," *Radio Science*, vol. 37, no. 4, pp. 1–1–1–22, 2002. [Online]. Available: https://agupubs.onlinelibrary.wiley.com/doi/abs/10.1029/2000RS002508
[19] C. Balanis, *Antenna Theory: Analysis and Design*. Wiley, 2012. [Online]. Available: https://books.google.hr/books?id=v1PSZ48DnuEC
[20] ICNIRP, "Guidelines for limiting exposure to electromagnetic fields (100 khz to 300 ghz)," *Health Physics*, vol. 5, no. 118, pp. 483–524, May 2020.

Zoran Blažević was born in Split, 1968. He received his BS degree in 1993, MS degree in 2000 and PhD in 2005 at the University of Split, Faculty of Electrical Engineering, Mechanical Engineering and Naval Architecture, Split; Croatia. For six years he was with Croatian Railways as a telecommunication engineer. Currently he is Full Professor at the Department of Electronics, leading a number of courses in the area of radio on the graduate study of information and communication technology. He was involved in organization and execution of several international conferences as an organizer or technical committee member, and several national science projects as a project leader or researcher. He appears as an author or coauthor of more than 100 journal and conference papers and two book chapters in the area of radio systems, channel modeling, radio-propagation and microwaves.

Maja Škiljo received her PhD in 2014 from the University of Split, Faculty of Electrical Engineering, Mechanical Engineering and Naval Architecture (FESB), where she is currently an Associate Professor. Her research interests include wireless power transfer, antennas and propagation, electromagnetic compatibility, radar systems, and the Internet of Things (IoT). She has co-authored more than 50 publications in international journals and conference proceedings, as well as a book chapter. She has participated as a research member in several funded research projects and is currently involved in two projects supported by the Croatian Science Foundation. She is a member of CCIS, IEEE, and the IEEE Electromagnetic Compatibility Society, and served as President of the IEEE EMC Croatia Chapter from 2024 to 2025.

Dragan Poljak (SM' 13) received his PhD in el. Eng. in 1996 from the Univ. of Split, Croatia. He is the Full Prof. at Dept. of Electron. and Computing, Univ. of Split. His research interests are oriented to computational electromagnetics (electromagn. compatibility, bioelectromagnetics and plasma physics). To date Prof. Poljak has published more than 160 journ. and 250 conf. papers, and authored some books, e.g. two by Wiley, one by IEEE and one by Elsevier. He is a Senior member of IEEE, a member of Editorial Board of Eng. Anal. with Boundary Elements, Math. Problems in Eng. And IET Sci. Measur. & Techn. He was awarded by several prizes for his achievements, such as National Prize for Science (2004) and (2023), Croatian sect. of IEEE annual Award (2016), Technical Achievement Award of the IEEE EMC Society (2019) and George Green Medal from University of Mississippi (2021). From May 2013 to June 2021 Prof. Poljak was a member of the board of the Croatian Science Foundation. He is currently involved in ITER physics and DONES EUROfusion collab. and in Croatian center for excellence in research for tech. sciences. He is active in few Working Groups of IEEE/Internat. Committee on Electromagnetic Safety (ICES) Tech. Comm. 95 SC6 EMF Dosimetry Modeling.